SCIENTIFIC REPORTS

OPEN

SUBJECT AREAS:
PHYSICS
ELECTRONIC PROPERTIES AND MATERIALS

Received
11 September 2014

Accepted
1 December 2014

Published
23 December 2014

Correspondence and requests for materials should be addressed to L.G. (lukegordon@engineering.ucsb.edu) or C.G.V.d.W. (vandewalle@mrl.ucsb.edu)

Hydrogen bonds in Al_2O_3 as dissipative two-level systems in superconducting qubits

Luke Gordon, Hazem Abu-Farsakh, Anderson Janotti & Chris G. Van de Walle

Materials Department, University of California, Santa Barbara, CA 93106-5050, USA.

Dissipative two-level systems (TLS) have been a long-standing problem in glassy solids over the last fifty years, and have recently gained new relevance as sources of decoherence in quantum computing. Resonant absorption by TLSs in the dielectric poses a serious limitation to the performance of superconducting qubits; however, the microscopic nature of these systems has yet to be established. Based on first-principles calculations, we propose that hydrogen impurities in Al_2O_3 are the main source of TLS resonant absorption. Hydrogen is an ubiquitous impurity and can easily incorporate in Al_2O_3. We find that interstitial H in Al_2O_3 forms a hydrogen bond (O-H…O). At specific O-O distances, consistent with bond lengths found in amorphous Al_2O_3 or near Al_2O_3 surfaces or interfaces, the H atom feels a double well. Tunneling between two symmetric positions gives rise to resonant absorption in the range of 10 GHz, explaining the experimental observations. We also calculate the expected qubit-TLS coupling and find it to lie between 16 and 20 MHz, consistent with experimental measurements.

The existence of dissipative two-level systems (TLSs), typically observed in amorphous solids, is a long-standing problem in solid-state physics[1,2], but specific microscopic models have been lacking. A new impetus for uncovering their origins has emerged with the advance of qubits based on superconducting Josephson tunnel junctions[3,4]. Dissipation in the qubit causes the excited $|1>$ state to decay to the $|0>$ ground state, leading to decoherence[5,6]. Two-level systems (TLS) in the insulating layer have been reported to be a major source of energy loss[7]; this mechanism seems to dominate other sources of decoherence.

Dielectric loss from TLS can be large in amorphous materials (see Pohl *et al.*[8] for a detailed survey), and is thought to arise from random bonding of atoms. In superconducting qubits, TLSs are a source of decoherence in the tunnel barrier of the Josephson junction. Loss arises from absorption of microwave radiation by TLSs with an electric dipole moment. It can be modeled as atoms tunneling between two distinct positions[7], and has been shown to be important even for the surface oxide of superconducting metals (Al_2O_3)[9]. The effect of decoherence can be mitigated by the use of single-crystal Al_2O_3; a reduction in the density of spectral splittings of up to 80% has been observed[10]. The defects have resonance frequencies on the order of 10 GHz[7], comparable to the qubit circuit; the coupling strengths and decoherence times are sufficiently large for coherent oscillations between the qubit and TLS. Despite extensive studies on the physics and effects of TLSs[1,2,12], their microscopic origin has remained unsettled.

Here we show that TLSs in Al_2O_3 can be attributed to hydrogen impurities that incorporate on interstitial sites. Hydrogen is an ubiquitous impurity, present in many growth and processing environments, and able to unintentionally incorporate in most materials[13], including the Al_2O_3 dielectric used in superconducting qubits. The specific characteristics of hydrogen that give rise to the TLS are related to its propensity for hydrogen bonding; by definition it is the only element that exhibits this type of chemical bond. Interstitial hydrogen in oxides exhibits a strong, mainly covalent bond with a primary O atom, with a typical O-H bond length of ~1 Å, but can also interact with a next-nearest-neighbor (*nnn*) O atom, resulting in an O-H…O configuration[14,15]. For suitable O-O distances, the interaction with the *nnn* O atom leads to quantum-mechanical tunneling between these neighboring sites. Tunneling of interstitial hydrogen between adjacent O sites has been observed in oxides such as $KTaO_3$, for which Spahr *et al.*[16] reported tunneling rates in the 7–40 GHz range. We will demonstrate, based on first-principles theory, that hydrogen in Al_2O_3 can give rise to TLSs with tunneling frequencies that explain the dielectric loss observed in superconducting qubits.

The process of quantum-mechanical tunneling of interstitial hydrogen is complicated by the strong interactions of hydrogen with the lattice, which lead to relaxations of the host[17]. In its most stable configuration, the

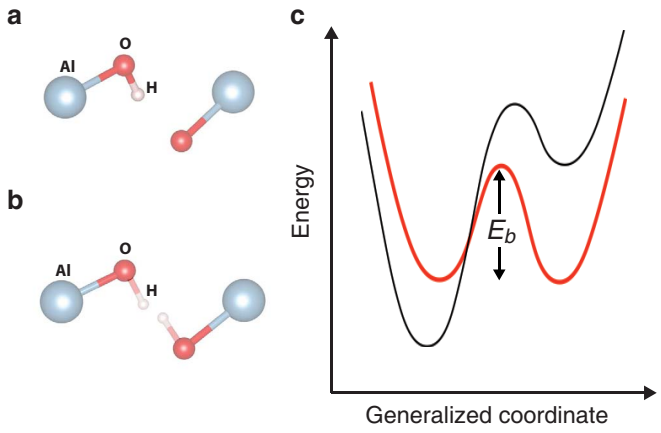

Figure 1 | Self-trapped and coincidence configurations. (a) Geometry of the self-trapped configuration for a hydrogen interstitial in Al_2O_3. H is bonded primarily to a specific O atom, but could alternatively be bonded to a *nnn* O atom. Al atoms are represented by large (grey) spheres, O atoms by smaller (red) spheres, and H atoms by the smallest (pink) spheres. (b) Geometry of a coincidence configuration, obtained by averaging over two adjacent self-trapped configurations. The two symmetric hydrogen sites are indicated by semi-transparent bonds. (c) Schematic potential-energy curve for the self-trapped (black) versus the coincidence (red) configurations. The latter corresponds to a double-well system with energy barrier E_b.

interstitial H is primarily bonded to one O atom, with a larger distance to the *nnn* O (Fig. 1a). In this atomic configuration, the metastable minimum at the *nnn* O is significantly higher in energy, or even nonexistent, when compared to the ground-state minimum. To enable tunneling, the lattice must be brought into a symmetric *coincidence configuration*[17,18] (Fig. 1b) where a double-well potential occurs and tunneling can take place (Fig. 1c). The three-dimensional (3D) potential energy surface corresponding to the coincidence configuration determines the energy levels and tunnel splittings for the quantum-mechanical motion of the H atom. These energy levels and tunneling frequencies can be calculated by numerically solving Schrödinger's equation. The determination of the coincidence configuration and the corresponding potential energy surface is an important aspect of the present work, discussed in detail below. We note that considering a purely adiabatic process, in which the host atoms assume their lowest-energy positions for each location of the H atom, is unrealistic due to the large mass difference between H and the other atoms. On the other hand, fixing the host atoms to positions corresponding to an unrelaxed lattice, or to those for the ground-state configuration of interstitial H, is unrealistic as well. We address this by employing a novel interpolation scheme between the ground state-minima at two adjacent O atoms, and we repeat this for different O-O distances in order to explore the properties of H in a wide range of possible coincidence configurations.

Results

Interstitial H in α-Al_2O_3 can assume three different charge states: positive (H_i^+), neutral (H_i^0), and negative (H_i^-). These configurations are calculated within density functional theory (DFT) using a screened hybrid functional (see Methods). The use of a hybrid functional is absolutely essential for properly describing the interaction between H and the *nnn* O atom, and thus the tunneling frequencies of the associated TLS. DFT within the standard generalized gradient approximation (GGA) overestimates the strength of the interaction between H and the *nnn* O atom so that the calculated O-H frequency is too low[19]. For the neutral and negative charge states, the interstitial hydrogen occupies a position in between two Al atoms, as shown in Fig. 2a,b. H_i^+, on the other hand, bonds to an O atom with a bond length of 1.01 Å, and a distance of 1.70 Å to the *nnn* O (Fig. 1c, 3b). The relative stability of the different charge states depends on the Fermi-level position. The formation energy of an interstitial H in charge state q $\left[E^f\left(H_i^q\right)\right]$ is calculated as[20]

$$E^f\left(H_i^q\right) = E_{\rm tot}\left(H_i^q\right) - E_{\rm tot}(Al_2O_3) - \mu_{\rm H} + q\epsilon_F, \qquad (1)$$

where $E_{\rm tot}\left(H_i^q\right)$ is the total energy of the supercell containing an interstitial H atom in charge state q, $E_{\rm tot}(Al_2O_3)$ is the total energy of the bulk supercell, $\mu_{\rm H}$ is the hydrogen chemical potential, and ϵ_F is the Fermi level, referenced to the valence-band maximum (VBM). The value of μ_H does not affect the relative stability of the different configurations, and we can set μ_H equal to half the total energy of an isolated H_2 molecule.

The calculated formation energies as a function of ϵ_F are shown in Fig. 3. We find that the donor state, H_i^+, is the stable charge state for Fermi levels up to 5.9 eV above the VBM; above that, the acceptor state, H_i^-, is most stable. The neutral charge state, H_i^0, is always higher in energy than both the H_i^+ and H_i^-, reflecting a negative-U character, as observed for H_i in many other semiconductors and insulators[13]. The position of the Fermi level is determined by charge neutrality; in an undoped α-Al_2O_3 crystal, native defects lead to a Fermi-level position around the middle of the gap[21]. Under these conditions, Fig. 3 shows that interstitial hydrogen is most stable in the positive charge state, H_i^+.

The relaxed geometry of the H_i^+ configuration in Al_2O_3 at its equilibrium volume is asymmetric, with significant relaxations of the host atoms, particularly of the O atom to which it is bonded (Fig. 2c). The energy difference between the unrelaxed Al_2O_3 lattice containing an H_i^+ and the relaxed lattice with H_i^+ in its most stable configuration is defined as the self-trapping energy[18,22], and is approximately 1.5 eV. One would expect this large energy difference to prohibit H from tunneling. In order to enable tunneling, a configuration must be created in which the hydrogen is equally likely to be bonded to either of the two neighboring O atoms. The lowest energy required to take a self-trapped configuration into a symmetric structure, i.e., the coincidence configuration, is the "coincidence energy" E_c. The formation of a coincidence geometry may be assisted by lattice vibrations, or may occur in regions where the atomic arrangement deviates from that in the bulk crystal, such as near surfaces or interfaces, or in an amorphous phase, in which a range of O-O distances from around 2.4 Å to 2.8 Å are observed[23–25].

An exact determination of the coincidence geometry would in principle require a self-consistent treatment of the quantum-mechanical hydrogen motion coupled to the host-atom relaxation[26], something that is too computationally demanding to be performed in conjunction with a first-principles treatment of the electronic structure. Approximate methodologies for obtaining the coincidence geometry have therefore been developed. Here we determine the coincidence configuration by averaging the positions of the host atoms for two self-trapped configurations, corresponding to H bonded to adjacent O sites. This procedure produces a symmetric double well potential for the tunneling hydrogen atom. We then place a H atom $\left(H_i^+\right)$ in the structure formed by the host atoms in the coincidence geometry and allow the hydrogen to relax (keeping the host atoms fixed). The energy difference between the relaxed H_i^+ in the coincidence geometry and the H_i^+ in the most stable, self-trapped configuration is the coincidence energy E_c.

We determined the coincidence configurations and coincidence energies for a range of different volumes of α-Al_2O_3, from equilibrium to 6% isotropic (linear) strain. This variation in lattice parameters corresponds to O-O distances between 2.715 to 2.59 Å in the perfect crystal, a range which includes the O-O distances found in amorphous Al_2O_3[23–25]. The corresponding O-O distance in the coincidence configuration varies in the range of 2.56 to 2.45 Å. The results are listed in Table 1 and shown in Fig. 4. The coincidence energies

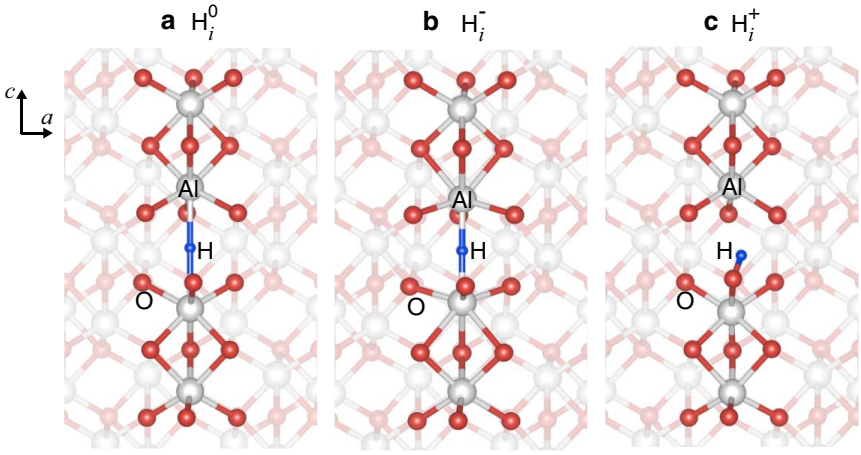

Figure 2 | Geometry of self-trapped hydrogen configuration in Al_2O_3. Relaxed "self-trapped" geometry of interstitial H in the (a) neutral, (b) negative, and (c) positive charge states. Al atoms are represented by large (grey) spheres, O atoms by smaller (red) spheres, and H atoms by the smallest (blue) spheres.

vary from 0.36 to 0.25 eV, with a minimum at 4% compression, corresponding to an O-O distance (in the coincidence geometry) of 2.49 Å.

The solution of Schrödinger's equation for the H atom in the 3D potential energy surface corresponding to the coincidence geometry produces wave functions and energies characteristic of a double-well potential. The tunnel splitting is calculated from the energy difference between the ground state and the first excited state, and leads to the tunneling frequencies listed in Table 1. In order to enable direct comparison to experiments, we have also calculated the qubit-TLS coupling strength for each possible configuration. The measured signal of a TLS in a phase qubit reflects the resonance between the splitting energy E_{01} and the tunnel splitting of the TLS, expressed as the qubit-TLS coupling strength S_{Max}. As described in the Methods section, S_{Max} is a function of the splitting E_{01} and the dipole moment p. We have calculated this quantity using experimental values for the qubit frequency (5.4 GHz, ref. 27) and for the capacitance and gate width, resulting in values between 16 and 20 MHz (Table 1).

Discussion

The results in Table 1 indicate that the tunneling frequencies are sensitive to the O-O distance, albeit not in a straightforward manner. Compression of the lattice initially makes little difference to the tunneling frequency, which remains around the value of 50 GHz

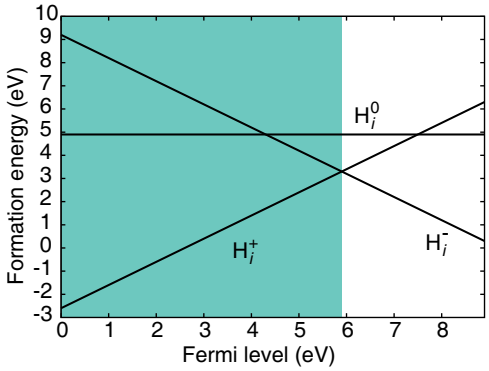

Figure 3 | Formation energy of H in Al_2O_3. Formation energy, calculated with hybrid density functional theory, of various charge states of interstitial hydrogen in α-Al_2O_3 as a function of Fermi level. The shaded area indicates the region of Fermi-level values in which H forms a hydrogen bond.

calculated for the equilibrium volume (see Fig. 4). The higher values of E_c (compared to those calculated at compressed volumes) suppress the possibility of tunneling in this regime. At 4.5% compression, corresponding to an O-O distance of 2.59 Å in the impurity-free crystal, the O-O distance in the coincidence configuration is 2.48 Å and the tunneling frequency is 16 GHz. Further compression of the lattice leads to a decrease in the potential barrier between the wells in the double well potential, and thus an increase in the tunneling frequency, away from the range observed in experiment. Such small O-O distances also have a decreased probability of occurring in actual samples.

Experimentally, a range of TLS tunneling frequencies have been reported, centered around 10 GHz[7,28]. To further corroborate our model, we can also compare our calculated qubit-TLS coupling constants S_{Max} to experiment. Reported values range from 25 MHz to 45 MHz[28,29]. The agreement with our calculated values (16–20 MHz, Table 1) further validates our claim that hydrogen is responsible for TLS decoherence in the dielectric layer.

The presence of hydrogen in dielectrics is highly plausible, particularly when they are deposited or grown using hydrogen-containing precursors. Hydrogen has been observed with secondary ion mass spectrometry (SIMS) in atomic-layer-deposited oxides[30]. Unfortunately, accurate experimental detection of hydrogen is fraught with difficulty, at least at the low concentrations and in the small volumes that are relevant for qubits. A decrease in loss has been reported in the case of crystalline dielectrics[10]. This is consistent with our results for crystalline α-Al_2O_3 at equilibrium volume, in which the tunneling frequencies are well outside the range that is relevant for the qubits. However, even in devices that use crystalline dielectrics, there is still a range of O-O distances at surfaces and interfaces[11], so TLS losses are never completely eliminated.

The results reported here are distinct from recent work by Holder *et al.*[12], also based on hybrid density functional theory, which considered the rotor motion of a H atom in α-Al_2O_3, either as an interstitial or in the Al vacancy. They concluded that interstitial hydrogen could not be responsible for TLSs, based on a value for the calculated tunneling frequency that was much higher than experiment. They did find one defect displaying frequencies in the GHz range, namely a complex of H with an Al vacancy in the +1 charge state. However, this complex is stable only if the Fermi level is within 1.2 eV of the VBM, which is highly unlikely (essentially impossible) in α-Al_2O_3, a wide-band-gap insulator. The frequency calculated for H_i^+ in Ref. 12 (~240 GHz) is significantly higher than the values reported here, likely stemming from their highly simplified 1D model. Our own tests have indicated that a full mapping of the 3D potential energy

Table 1 | Calculated TLS parameters for H in Al_2O_3. Coincidence energies E_c, tunnel splittings Δ, tunneling frequencies ν, and coupling constants S_{Max} for two-level systems associated with interstitial hydrogen in α-Al_2O_3. Values are listed for various O-O distances d_{O-O} ranging from 2.56 Å to 2.45 Å, corresponding to volume compression by the specified amounts

compression	d_{O-O} (Å)	E_c (eV)	Δ (eV)	ν (GHz)	S_{Max} (MHz)
0%	2.56	0.36	2.20×10^{-4}	53	19.8
1%	2.55	0.35	2.09×10^{-4}	50	18.3
2%	2.53	0.33	2.48×10^{-4}	59	19.2
3%	2.51	0.32	2.17×10^{-4}	53	17.1
3.5%	2.50	0.29	1.38×10^{-4}	33	16.7
4%	2.49	0.25	1.07×10^{-4}	26	16.4
4.5%	2.48	0.28	6.7×10^{-5}	16	16.4
5%	2.47	0.28	4.12×10^{-4}	90	16.3
6%	2.45	0.26	1.57×10^{-3}	360	16.0

surface is essential in Al_2O_3, and that 1D models do not match the full results. In addition, the sixfold or threefold degeneracies assumed in the rotor model of Ref. 12 are extremely unlikely to occur in real materials—even in crystalline solids. In contrast, the two-fold degeneracy inherent in our hydrogen-related double-well systems is highly plausible and fits within the general framework of two-level systems.

In summary, we have proposed a microscopic model for TLSs in Al_2O_3 based on interstitial hydrogen in an O-H…O hydrogen-bonding configuration. Hybrid DFT calculations produce frequencies that are in the range reported for TLSs known to be responsible for the main loss in superconducting qubits, and calculated qubit-TLS coupling paramaters are close to experimental values. We suggest that hydrogen could be responsible for TLSs in other materials as well, given its ubiquity. As the only element to exhibit "hydrogen bonding", it stands out as a candidate for TLSs in oxides, in which a range of suitable O-O distances occur. The low migration barriers observed (and calculated) for interstitial H^+ suggest that barriers between equivalent sites can be low enough to lead to significant tunneling and hence double-well systems.

Methods

Our calculations are based on density functional theory (DFT)[31,32] and the screened hybrid functional of Heyd, Scuseria, and Ernzerhof (HSE)[33,34] as implemented in the VASP code[35]. In the HSE functional the exchange potential is split into short- and long-range parts, with the range separation determined through an error function with a characteristic screening length of 10 Å. In the short-range region, the exchange potential of Perdew, Burke and Ernzerhof (PBE)[36] is mixed with the non-local Hartree-Fock exchange potential. The long-range region is described by the PBE functional, and so is the correlation potential. We use a Hartree-Fock mixing parameter of 32%, chosen to correctly describe the band gap of α-Al_2O_3[38]. The impurity calculations were performed using a supercell containing 120 atoms; this is a $2 \times 2 \times 1$ multiplier of the 30-atom unit cell of α-Al_2O_3. We used a $2 \times 2 \times 1$ Monkhorst-Pack **k**-point mesh for the integrations over the Brillouin zone, and a cutoff of 500 eV for the plane-wave basis set. Our HSE calculations for α-Al_2O_3 produce lattice parameters $a = b = 4.74$ Å and $c = 12.95$ Å, in very good agreement with the experimental values, $a = b = 4.76$ Å and $c = 12.99$ Å[37].

We study a variety of O-O interatomic distances (representative of those occurring in the amorphous phase or near surfaces or interfaces) by varying the volume of the crystalline solid, up to a total volumetric compression of 6%. The physics of the TLS studied here is determined by the local environment of the hydrogen atom, for which the presence (or absence) of long-range order is irrelevant. Our results for crystalline α-Al_2O_3 therefore also apply to amorphous Al_2O_3, in which the relevant O-O interatomic distances occur, as evidenced by pair-correlation distributions[23–25].

The 3D potential energy surface for the H atom in the host lattice (fixed to the coincidence configuration) was determined by calculating the total energy for each point on a grid with a spacing of 0.24 Å in the three spatial directions. This grid was then interpolated using the energy gradients obtained from the forces acting on the H atom, leading to a smooth function. To numerically solve the Schroödinger's equation for the quantum-mechanical motion of H, the wave functions were expanded in a plane-wave basis set with a cutoff energy of 800 eV; this cutoff was determined based on convergence tests for the tunnel splittings.

The qubit-TLS coupling S_{Max} can be calculated as[7, 39]

$$S_{Max} = \frac{2p}{x}\sqrt{e^2 E_{01}}2C, \tag{2}$$

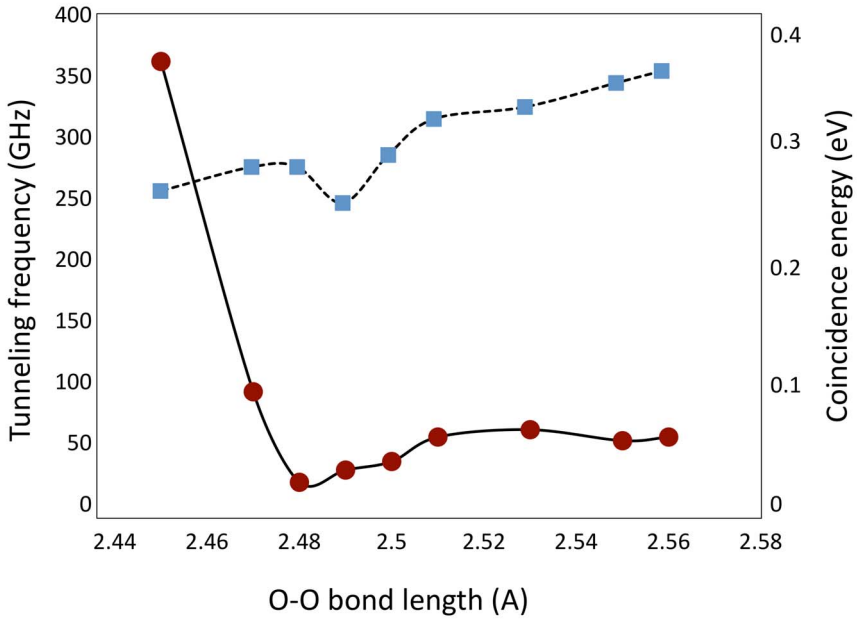

Figure 4 | Tunneling frequency as a function of O-O distance. Calculated tunneling frequencies and coincidence energies are shown for O-O distances ranging from 2.45 to 2.56 Å in the coincidence geometry. Tunneling frequencies are shown in red, coincidence energies in blue.

where x is the barrier thickness, p is the effective dipole moment of the charge in the double-well system, C is the capacitance, and E_{01} is the qubit splitting energy. We assume a junction width $x = 2$ nm, a capacitance $C = 850$ fF, and a qubit splitting energy 5.4 GHz, corresponding to representative experimental values[27,28]. The dipole moment is calculated as the product of the effective charge around the hydrogen atom in the coincidence configuration and the distance between the symmetric potential wells, determined from first-principles calculations.

1. Philips, W. A. Two-level states in glasses. *Rep. Prog. Phys.* **50**, 1657 (1987).
2. Leggett, A. J. *et al*. Dynamics of the dissipative two-state system. *Rev. Mod. Phys.* **59**, 1 (1987).
3. Steffen, M. Superconducting qubits are getting serious. *Physics* **4**, 103 (2011).
4. Barends, R. *et al*. Superconducting quantum circuits at the surface code threshold for fault tolerance. *Nature* **508**, 500 (2014).
5. Collin, E. *et al*. NMR-like control of a quantum bit superconducting circuit. *Phys. Rev. Lett.* **93**, 157005 (2004).
6. Astafiev, O. *et al*. Quantum noise in the Josephson charge qubit. *Phys. Rev. Lett.* **93**, 267007 (2004).
7. Martinis, J. M. *et al*. Decoherence in Josephson qubits from dielectric loss. *Phys. Rev. Lett.* **95**, 210503 (2005).
8. Pohl, R. O., Liu, X. & Thompson, E. Low-temperature thermal conductivity and acoustic attenuation in amorphous solids. *Rev. Mod. Phys.* **74**, 991 (2002).
9. Gao, J. *et al*. Experimental evidence for a surface distribution of two-level systems in super-conducting lithographed microwave resonators. *Appl. Phys. Lett.* **92**, 152505 (2008).
10. Oh, S. *et al*. Elimination of two level fluctuators in superconducting quantum bits by an epitaxial tunnel barrier. *Phys. Rev. B* **74**, 100502 (2006).
11. Pilania, G. *et al*. Revisiting the Al/Al2O3 interface: Coherent interfaces and misfit accommo-dation. *Sci. Rep.* **4**, 4485 (2014).
12. Holder, A. M., Osborn, K. D., Lobb, C. J. & Musgrave, C. B. Bulk and surface tunneling hydrogen defects in alumina. *Phys. Rev. Lett.* **111**, 065901 (2013).
13. Van de Walle, C. G. & Neugebauer, J. Universal alignment of hydrogen levels in semiconductors, insulators and solutions. *Nature* **423**, 626 (2003).
14. Novak, A. Hydrogen bonding in solids. Correlation of spectroscopic and crystallographic data. *Structure and Bonding* **18**, 177 (1974).
15. Hlaing Oo, W. M. *et al*. Hydrogen donors in SnO_2 studied by infrared spectroscopy and first-principles calculations. *Phys. Rev. B* **82**, 193201 (2010).
16. Spahr, E. J. *et al*. Proton Tunneling: A decay channel of the O-H stretch mode in $KTaO_3$. *Phys. Rev. Lett.* **102**, 075506 (2009).
17. Flynn, C. P. & Stoneham, A. M. Quantum theory of diffusion with application to light interstitials in metals. *Phys. Rev. B* **1**, 3966 (1970).
18. Sundell, P. G. & Wahnstrom, G. Activation energies for quantum diffusion of hydrogen in metals and on metal surfaces using delocalized nuclei within the density-functional theory. *Phys. Rev. Lett.* **92**, 155901 (2004).
19. Johnson, B. G., Gill, P. M. W. & Pople, J. A. The performance of a family of density functional methods. *J. Chem. Phys.* **98**, 5612 (1993).
20. Freysoldt, C. *et al*. First-principles calculations for point defects in solids. *Rev. Mod. Phys.* **86**, 253 (2014).
21. Choi, M., Lyons, J. L., Janotti, A. & Van de Walle, C. J. Impact of native defects in high-k dielectric oxides on GaN/oxide metaloxidesemiconductor devices. *Phys. Status Solidi B* **250**, 787 (2013).
22. Sundell, P. G., Bjorketun, M. E. & Wahnstrom, G. Density-functional calculations of prefactors and activation energies for H diffusion in $BaZrO_3$. *Phys. Rev. B* **76**, 094301 (2007).
23. Vashishta, P., Kalia, R. K., Nakano, A. & Pedro Rino, J. Molecular dynamics simulation studies of amorphous and liquid alumina. *J. Appl. Phys.* **103**, 083504 (2008).
24. Lamparter, P. & Kniep, R. Structure of amorphous Al_2O_3. *Physica B* **234**, 405 (1997).
25. Davis, S. & Gutierrez, G. Structural, elastic, vibrational and electronic properties of amorphous Al_2O_3 from ab initio calculations. *J. Phys. Condens. Matter* **23**, 495401 (2011).
26. Miyake, T., Ogitsu, T. & Tsuneyuki, S. Quantum distributions of muonium and hydrogen in crystalline silicon. *Phys. Rev. Lett.* **81**, 1873 (1998).
27. Barends, R. *et al*. Coherent Josephson qubit suitable for scalable quantum integrated circuits. *Phys. Rev. Lett.* **111**, 080502 (2013).
28. Shalibo, Y. *et al*. Lifetime and coherence of two-Level defects in a Josephson junction. *Phys. Rev. Lett.* **105**, 177001 (2010).
29. Cole, J. H. *et al*. Quantitative evaluation of defect-models in superconducting phase qubits. *Appl. Phys. Lett.* **97**, 252201 (2010).
30. Khalil, M. S. *et al*. Evidence for hydrogen two-level systems in atomic layer deposition oxides. *Appl. Phys. Lett.* **103**, 162601 (2013).
31. Hohenberg, P. & Kohn, W. Inhomogeneous electron gas. *Phys. Rev.* **136**, B864 (1964).
32. Kohn, W. & Sham, L. J. Self-consistent equations Including exchange and correlation effects. *Phys. Rev.* **140**, A1133 (1965).
33. Heyd, J., Scuseria, G. E. & Ernzerhof, M. Hybrid functionals based on a screened Coulomb potential. *J. Chem. Phys.* **118**, 8207 (2003).
34. Heyd, J., Scuseria, G. E. & Ernzerhof, M. Erratum: Hybrid functionals based on a screened Coulomb potential [J. Chem. Phys. 118, 8207 (2003)]. *J. Chem. Phys.* **124**, 219906 (2006).
35. Kresse, G. & Furthmuller, J. Efficient iterative schemes for *ab initio* total-energy calculations using a plane-wave basis set. *Phys. Rev. B.* **54**, 11169 (1996).
36. Perdew, J. P., Burke, K. & Ernzerhof, M. Generalized gradient approximation made simple. *Phys. Rev. Lett.* **77**, 3865 (1996).
37. Ball, C. J. Determination of lattice parameters from synchrotron powder data: A study using high temperature data for tungsten and alumina. *Powder Diffraction* **21**, 1 (2006).
38. Wang, Z., Li, C., Liu, L. & Sham, T. Electronic Structures and Optical Properties of -Al2O3 Nanowires. *Journal of Physics: Conference Series* **430**, 012065 (2013).
39. DuBois, T. C., Per, M. C., Russo, S. P. & Cole, J. H. Delocalized oxygen as the origin of two-Level defects in Josephson junctions. *Phys. Rev. Lett.* **110**, 077002 (2013).

Acknowledgments

We gratefully acknowledge valuable discussions with J. Martinis. This work was supported by IARPA through the U. S. Army Research Office (Grant No. W911NF-09-1-0375). Computational resources were provided by the Center for Scientific Computing at the CNSI, MRL (an NSF MRSEC, DMR-1121053) and NSF CNS-0960316, and by the Extreme Science and Engineering Discovery Environment (XSEDE), supported by NSF ACI-1053575 (TG-DMR070072N).

Author contributions

L.G., H.A.F., A.J. and C.G.V.d.W. designed and performed all research. L.G., A.J. and C.G.V.d.W. wrote the main manuscript text.

Additional information

Competing financial interests: The authors declare no competing financial interests.

How to cite this article: Gordon, L., Abu-Farsakh, H., Janotti, A. & Van de Walle, C.G. Hydrogen bonds in Al_2O_3 as dissipative two-level systems in superconducting qubits. *Sci. Rep.* **4**, 7590; DOI:10.1038/srep07590 (2014).